

Observational and Model Estimates of Cloud Amount Feedback over the Indian and Pacific Oceans

KATINKA BELLOMO AND AMY C. CLEMENT

Rosenstiel School of Marine and Atmospheric Science, University of Miami, Miami, Florida

JOEL R. NORRIS

Scripps Institution of Oceanography, University of California, San Diego, La Jolla, California

BRIAN J. SODEN

Rosenstiel School of Marine and Atmospheric Science, University of Miami, Miami, Florida

(Manuscript received 13 March 2013, in final form 16 September 2013)

ABSTRACT

Constraining intermodel spread in cloud feedback with observations is problematic because available cloud datasets are affected by spurious behavior in long-term variability. This problem is addressed by examining cloud amount in three independent ship-based [Extended Edited Cloud Reports Archive (EECRA)] and satellite-based [International Satellite Cloud Climatology Project (ISCCP) and Advanced Very High Resolution Radiometer Pathfinder Atmosphere-Extended (PATMOS-X)] observational datasets, and models from phase 5 of the Coupled Model Intercomparison Project (CMIP5). The three observational datasets show consistent cloud variability in the overlapping years of coverage (1984–2007). The long-term cloud amount change from 1954 to 2005 in ship-based observations shares many of the same features with the multimodel mean cloud amount change of 42 CMIP5 historical simulations, although the magnitude of the multimodel mean is smaller. The radiative impact of cloud changes is estimated by computing an observationally derived estimate of cloud amount feedback. The observational estimates of cloud amount feedback are statistically significant over four regions: the northeast Pacific subtropical stratocumulus region and equatorial western Pacific, where cloud amount feedback is found to be positive, and the southern central Pacific and western Indian Ocean, where cloud amount feedback is found to be negative. Multimodel mean cloud amount feedback is consistent in sign but smaller in magnitude than in observations over these four regions because models simulate weaker cloud changes. Individual models, however, can simulate cloud amount feedback of the same magnitude if not larger than observed. Focusing on the regions where models and observations agree can lead to improved understanding of the mechanisms of cloud amount changes and associated radiative impact.

1. Introduction

Cloud feedback represents the largest uncertainty of future climate change in climate models from phase 3 of the Coupled Model Intercomparison Project (CMIP3) used for the Intergovernmental Panel on Climate Change Fourth Assessment Report (IPCC AR4) (Solomon et al. 2007; Soden and Held 2006; Ringer et al. 2006; Dufresne and Bony 2008; Trenberth and Fasullo 2009; Stephens

2005). Intermodel disagreement in cloud feedback has been attributed to differences in cloud parameterization schemes and is largest for tropical low-level clouds (Bony et al. 2006, Webb et al. 2006), which are ubiquitous over the oceans (Norris 1998). Some components of cloud feedback, however, show intermodel agreement. For example, there is model agreement on the change in the altitude of tropical high-level cloud cover, which results in positive high cloud altitude feedback (Zelinka and Hartmann 2010). Hartmann and Larson (2002) proposed the fixed-anvil-temperature (FAT) mechanism to explain positive cloud altitude feedback. According to the FAT mechanism, high clouds in the tropics tend to rise as the climate warms in order to conserve their cloud-top temperature.

Corresponding author address: Katinka Bellomo, Rosenstiel School of Marine and Atmospheric Science, University of Miami, 4600 Rickenbacker Cswy., Miami, FL 33149.
E-mail: kbellomo@rsmas.miami.edu

This mechanism appears to be robust across climate models, and is consistent with the response of high clouds to El Niño events (Zelinka and Hartmann 2011).

Bony and Dufresne (2005) and Soden and Vecchi (2011) showed that the largest source of intermodel disagreement in tropical cloud feedback arises from the response of clouds in regions of large-scale subsidence over the tropical oceans. The subtropical stratocumulus regions at the eastern side of the ocean basins are among the regions of largest intermodel spread in cloud feedback among the CMIP3 models (Soden and Vecchi 2011). These regions are mainly covered by stratus and stratocumulus cloud types, which form over oceans with relatively cold sea surface temperature (SST), and to the east of the subtropical highs. Klein and Hartmann (1993) and subsequent studies have identified five major subtropical stratocumulus regions located off the coasts of Australia (southeast Indian), California (northeast Pacific), Peru (southeast Pacific), Canaries (northeast Atlantic), and Namibia (southeast Atlantic). In these regions, marine boundary layers are often well mixed and capped by strong temperature inversions. Increased cloud cover is associated with relatively cold SST, high lower tropospheric stability (LTS), large-scale atmospheric subsidence, and surface wind divergence (Klein and Hartmann 1993; Wood and Bretherton 2006; Klein et al. 1995; Muñoz et al. 2011). While strong subsidence generally coincides with strong LTS on seasonal to interannual time scales, individually these two quantities can have opposing effects on clouds. For example, Myers and Norris (2013) show that strong subsidence favors reduced cloud cover for the same LTS while stronger LTS promotes greater cloudiness for the same subsidence rate.

Given this complexity, simulating cloud variability in climate models is challenging. While observations show clear relationships between environmental variables and cloud fraction, the simulated relationships are highly model dependent (Clement et al. 2009). Moreover, in response to greenhouse gas forcing models project an increase in SST, which on its own would decrease low-level clouds (Brient and Bony 2013; Sandu and Stevens 2011), an increase in lower tropospheric stability, which would increase low-level clouds (Miller 1997; Medeiros et al. 2008), and weaker midtropospheric large-scale subsidence (Vecchi and Soden 2007a,b), which could either decrease low-level clouds (Sandu and Stevens 2011; Mauger and Norris 2010; Stevens et al. 2007) or increase them (Myers and Norris 2013). An observational perspective on long-term cloud changes could therefore provide an important constraint on cloud feedback simulated by the models and on mechanisms of cloud change.

Long-term cloud observations from synoptic ship reports are the longest source of cloud information and

could potentially narrow the uncertainties in climate models. However, only a few studies have looked at long-term changes in observations, mainly because of the artifacts that affect the available cloud datasets (Norris 1999; Eastman et al. 2011). Clement et al. (2009) examined cloud variability in the northeast Pacific subtropical stratocumulus region in multiple satellite and surface datasets. They found that cloud cover, SST, and large-scale atmospheric circulation covaried on decadal time scales, suggesting a positive feedback between stratocumulus clouds and large-scale Pacific climate variability. Eastman et al. (2011) examined low-level cloud cover changes in observations from ships over the years 1954–2008 in the subtropical stratocumulus regions. They found that decreased stratocumulus cloud cover was partially compensated by increased cumulus cloud cover, which suggests a long-term stratocumulus-to-cumulus transition and positive low-cloud feedback (Albrecht et al. 1995; Bretherton and Wyant 1997; Wood and Bretherton 2004; Sandu and Stevens 2011). Deser et al. (2010) examined long-term trends in cloud cover from 1900 to the present and found an eastward shift in cloud cover in the western Pacific that is consistent with a weakening of the Walker circulation. Norris (2005) investigated upper-level cloud trends in ship-based observations from 1954 to 1997. He found an increase in high clouds over the central equatorial South Pacific and a decrease over the adjacent subtropics, the western Pacific, and the equatorial Indian Ocean.

Despite the uncertainties in ship-based observational datasets, all the studies mentioned above showed that cloud changes were consistent with changes in precipitation, surface wind divergence, SST, sea level pressure (SLP), total-sky radiation flux anomalies, and satellite-based cloud observations in the overlapping period. In this study we will address the following questions: Are ship-based cloud observations reliable enough to constrain cloud feedback simulated by climate models? What is the radiative impact of the observed cloud changes? Can models reproduce the observed cloud change and cloud feedback? To address these questions we compare cloud cover changes in three observational ship- and satellite-based cloud datasets [the Extended Edited Cloud Reports Archive (EECRA), International Satellite Cloud Climatology Project (ISCCP), and Advanced Very High Resolution Radiometer Pathfinder (AVHRR) Atmosphere-Extended (PATMOS-X)] in the overlapping years of coverage. We estimate cloud amount feedback from long-term ship-based observations where they agree with satellites, and then compare these estimates with historical simulations from the phase 5 of the Coupled Model Intercomparison Project (CMIP5) archive (Taylor et al. 2012).

2. Data

We examine total cloud amount over the ocean in ship-based (EECRA) and satellite-based (ISCCP and PATMOS-X) cloud datasets. The Extended Edited Cloud Reports Archive is a collection of synoptic weather reports taken aboard volunteer observing ships (Hahn and Warren 1999, 2009). Reports of cloud cover are archived in the International Comprehensive Ocean–Atmosphere Data Set (ICOADS) (Woodruff et al. 2005, 2011), and then further processed to form EECRA, which currently provides cloud amount, cloud type, and frequency of occurrence, in $10^\circ \times 10^\circ$ grid boxes over the global oceans for the years 1954–2008 (Eastman et al. 2011). EECRA represents the longest source of cloud information, but it is affected by observational artifacts that introduce spurious trends in the global mean long-term variability (Norris 1999, 2005; Eastman et al. 2011).

To evaluate possible errors in EECRA, we supplement ship observations with two satellite-based cloud datasets: the International Satellite Cloud Climatology Project (Rossow and Schiffer 1999) and the AVHRR Pathfinder Atmosphere–Extended (PATMOS-X; Jacobowitz et al. 2003; Pavolonis et al. 2005). These datasets were corrected for artifacts introduced by the replacement of instruments and orbital drifts over time (Clement et al. 2009; Evan et al. 2007). Unknown remaining artifacts were corrected by subtracting global-scale long-term variability from each grid box (Evan et al. 2013). ISCCP and PATMOS-X provide monthly means of total cloud amount in $2.5^\circ \times 2.5^\circ$ grid boxes from June 1983 to July 2008.

To compute cloud amount feedback we use total cloud cover from EECRA along with radiation fluxes at the top of the atmosphere (TOA) and SST. Radiation fluxes at TOA are from the Clouds and Earth’s Radiant Energy System (CERES) Energy Balanced and Filled (EBAF) dataset (EBAF_Ed2.6r). This product is provided by the National Aeronautics and Space Administration (NASA) Langley Research Center and is available for the years 2001–10 in $1^\circ \times 1^\circ$ grid boxes (Loeb et al. 2009). For SST, we use the Hadley Centre Sea Ice and Sea Surface Temperature (HadISST) reanalysis, which is provided in $1^\circ \times 1^\circ$ grid boxes and is available from 1870 to today (Rayner et al. 2003).

We compare observational estimates of cloud change and cloud amount feedback with historical simulations of 42 coupled ocean–atmosphere climate models in the Coupled Model Intercomparison Project phase 5 (CMIP5) archive (Taylor et al. 2012). The historical simulations are forced by observed atmospheric composition changes and cover most of the industrial period from 1850 to 2005. We analyze one ensemble member (r1i1p1) for each model and examine the same years (1954–2005) covered

by ship observations. A list of the models used is provided in Table 1.

Total cloud fraction from observations, which is retrieved from visually or remotely measured optical depth, is not the same as total cloud fraction from models, which is computed from the model equations (e.g., Marchand et al. 2010). To provide a more accurate evaluation of model performance, cloud simulators have been developed (Klein et al. 2013; Pincus et al. 2012). Unfortunately there are not simulators of human observers (i.e., ship-based datasets), but we will show that intermodel spread in the sign of cloud changes is larger than errors that could arise from the different definitions of cloud cover in models and ship observations.

3. Methods

In this study, we focus on cloud changes over the tropical and subtropical Indian and Pacific basins. To correct long-term spurious variability in EECRA, we subtract the tropical annual mean from all years and all grid boxes. A similar approach was taken by Deser et al. (2010) to correct the ICOADS cloud dataset, which is affected by the same observational errors as EECRA since cloud observations in EECRA are processed from ICOADS. For consistency, we subtract the tropical annual mean from cloud observations in the corrected ISCCP and PATMOS-X datasets, and in the 42 CMIP5 historical simulations. Therefore, all results shown in this study should be interpreted as relative to the tropical mean. In the observational datasets, we also mask out poorly sampled regions by requiring an average of at least 25 observations per season in each grid box (cf. Eastman et al. 2011).

We form interannual anomalies by removing the seasonal cycle from all model and observational data, and then calculate long-term changes in cloud amount and SST as the linear trend in each grid box multiplied by the number of years. Estimates of cloud amount feedback are calculated as follows. Net (i.e., shortwave plus longwave) radiation flux at TOA (R_{tot}) can be expressed as the sum of overcast sky radiation (R_{cld}) with area c and clear-sky radiation (R_{clr}) with area $(1 - c)$, where c is the fraction of sky covered by clouds, and R_{tot} is positive for downwelling fluxes:

$$R_{\text{tot}} = cR_{\text{cld}} + (1 - c)R_{\text{clr}}. \quad (1)$$

The change in R_{tot} between two climate states can therefore be written as

$$\Delta R_{\text{tot}} = \Delta R_{\text{clr}} + \Delta c(R_{\text{cld}} - R_{\text{clr}}) + c(\Delta R_{\text{cld}} - \Delta R_{\text{clr}}) + \varepsilon. \quad (2)$$

TABLE 1. Forty-two ocean–atmosphere coupled climate models that provided the first ensemble member (r1i1p1) for the historical experiment in the CMIP5 archive.

Institution	Model name
Commonwealth Scientific and Industrial Research Organization (CSIRO) and Bureau of Meteorology (BOM) (Australia)	Australian Community Climate and Earth-System Simulator, version 1.0 (ACCESS1.0) ACCESS1.3
Beijing Climate Center, China Meteorological Administration (China)	Beijing Climate Center, Climate System Model, version 1.1 (BCC-CSM1.1) BCC-CSM1.1 with a moderate resolution [BCC-CSM1.1(m)] Beijing Normal University - Earth System Model (BNU-ESM)
College of Global Change and Earth System Science, Beijing Normal University (China)	
Canadian Centre for Climate Modeling and Analysis (Canada)	Second Generation Canadian Earth System Model (CanESM2)
National Center for Atmospheric Research (U.S.)	Community Climate System Model, version 4 (CCSM4)
Community Earth System Model (CESM) contributors (U.S.)	CESM version 1 (CESM1), biogeochemistry version (BGC) CESM1 with Community Atmosphere Model version 5 (CAM5) CESM1 with FASTCHEM (FASTCHEM) CESM1 with Whole Atmosphere Community Climate Model (WACCM)
Centre National de Recherches Meteorologiques/Centre Europeen de Recherche et Formation Avancees en Calcul Scientifique (France)	Centre National de Recherches Meteorologiques Coupled Global Climate Model, version 5 (CNRM-CM5) CNRM-CM5(2)
Commonwealth Scientific and Industrial Research Organization in collaboration with Queensland Climate Change Centre of Excellence (Australia)	Commonwealth Scientific and Industrial Research Organisation Mark, version 3.6.0 (CSIRO-Mk3.6.0)
LASG, Institute of Atmospheric Physics, Chinese Academy of Sciences and CESS, Tsinghua (China)	Flexible Global Ocean–Atmosphere–Land System Model gridpoint, version 2.0 (FGOALS-g2)
The First Institute of Oceanography, SOA (China)	First Institute of Oceanography Earth System Model (FIO-ESM)
NOAA Geophysical Fluid Dynamics Laboratory (U.S.)	Geophysical Fluid Dynamics Laboratory (GFDL) Climate Model, version 3 (GFDL-CM3) GFDL Earth System Model with Generalized Ocean Layer Dynamics (GOLD) component (GFDL-ESM2G) GFDL Earth System Model with Modular Ocean Model 4 (MOM4) component (GFDL-ESM2M)
NASA Goddard Institute for Space Studies (U.S.)	Goddard Institute for Space Studies (GISS) Model E, coupled with the HYCOM ocean model (GISS-E2-H) GISS-E2-H with interactive terrestrial carbon cycle and oceanic biogeochemistry (GISS-E2-H-CC) GISS Model E, coupled with the Russell ocean model (GISS-E2-R) GISS-E2-R with interactive terrestrial carbon cycle and oceanic biogeochemistry (Giss-E2-R-CC)
National Institute of Meteorological Research/Korea Meteorological Administration (South Korea)	Hadley Centre Global Environment Model, version 2 - Atmosphere and Ocean (HadGEM2-AO)
Met Office Hadley Centre (U.K.)	Hadley Centre Coupled Model, version 3 (HadCM3) Hadley Centre Global Environment Model, version 2 (HadGEM)–Carbon Cycle (HadGEM2-CC) HadGEM2–Earth System (HadGEM2-ES)
Institute for Numerical Mathematics (Russia)	Institute of Numerical Mathematics Coupled Model, version 4.0 (INM-CM4)
Institut Pierre-Simon Laplace (France)	L'Institut Pierre-Simon Laplace (IPSL) Coupled Model, version 5, coupled with NEMO, low resolution (IPSL-CM5A-LR) IPSL Coupled Model, version 5, coupled with NEMO, low resolution (IPSL-CM5A-MR) IPSL-CM5B-LR; new atmospheric physics at low resolution

TABLE 1. (Continued)

Institution	Model name
Atmosphere and Ocean Research Institute (The University of Tokyo), National Institute for Environmental Studies, and Japan Agency for Marine-Earth Science and Technology (Japan)	Model for Interdisciplinary Research on Climate (MIROC), Earth System Model (MIROC-ESM) MIROC, Earth System Model, Chemistry Coupled (MIROC-ESM-CHEM) MIROC, version 4 (high resolution) (MIROC4h) MIROC, version 5 (MIROC5)
Max Planck Institute for Meteorology (Germany)	Max Planck Institute (MPI) Earth System Model, low resolution (MPI-ESM-LR) MPI Earth System Model, medium resolution (MPI-ESM-MR) MPI Earth System Model, paleo (MPI-ESM-P)
Meteorological Research Institute (Japan)	Meteorological Research Institute (MRI) Coupled Atmosphere–Ocean General Circulation Model, version 3 (MRI-CGCM3) MRI Earth System Model, version 1 (MRI-ESM1)
Norwegian Climate Centre (Norway)	Norwegian Earth System Model, version 1 (intermediate resolution) (NorESM1-M) NorESM1 with prognostic biogeochemical cycling (NorESM1-ME)

The first term on the RHS of (2) represents the change in clear-sky flux. The second term represents the contribution from changes in cloud cover (Δc) with all the other properties affecting radiation held fixed, while the third term represents the effect of changes in radiation fluxes weighted by the mean cloud cover. The last term (ϵ) accounts for the covariance among the fields.

In previous studies observational estimates of cloud feedback have often been computed as the change in cloud radiative effect (CRE) at TOA divided by change in global mean SST (ΔT_s). The change in CRE at TOA can be written rearranging Eq. (2) as

$$\Delta \text{CRE} = \Delta R_{\text{tot}} - \Delta R_{\text{clr}} = \Delta c(R_{\text{cld}} - R_{\text{clr}}) + c(\Delta R_{\text{cld}} - \Delta R_{\text{clr}}), \quad (3)$$

where the covariance term is much smaller than the other terms and can be omitted (cf. Taylor et al. 2007). This method has been criticized because the second term on the RHS of (3) may include changes in clear-sky fluxes due to noncloud feedbacks (see discussion in Soden et al. 2008). These changes can cause a change in CRE that is not caused by a change in cloud cover.

In this study, we use only the first term on the RHS of (3) to define cloud feedback, so our definition is not contaminated by changes in clear-sky radiation. When this term [i.e., $\Delta c(R_{\text{cld}} - R_{\text{clr}})$] is divided by change in SST (ΔT_s) it represents cloud feedback. We note that we cannot evaluate cloud feedback due to changes in cloud vertical and optical properties because long-term ship-based observations only provide information about cloud amount. Therefore, Δc in our study corresponds to changes

in cloud amount and we can only estimate the cloud amount component of cloud feedback.

Since CRE is defined as $\text{CRE} = R_{\text{tot}} - R_{\text{clr}}$, we can write $R_{\text{cld}} - R_{\text{clr}}$ using (1) as

$$k = \frac{\overline{\text{CRE}}}{\bar{c}}, \quad (4)$$

where k represents the sensitivity of R_{tot} to changes in cloud amount, and is calculated as mean cloud radiative effect ($\overline{\text{CRE}} = \overline{R_{\text{tot}} - R_{\text{clr}}}$) at TOA from CERES divided by mean cloud amount (\bar{c}) from EECRA. We will refer to k as “cloud amount radiative kernel” in the remainder of this text in analogy to cloud radiative kernels developed by Zelinka et al. (2012a). In previous studies, k has been evaluated using a radiative transfer model that calculates cloud radiative kernels directly (Zelinka et al. 2012a; Zhou et al. 2013) or as a residual from radiative kernels of all the other noncloud feedback variables (Soden et al. 2008). Other methods have also been developed [e.g., the “approximate partial radiative perturbation method” of Taylor et al. (2007)]. Soden et al. (2008) provide a good overview of these different techniques. In addition to changes in cloud amount, these methods generally take into account the sensitivity to perturbations in cloud vertical and optical properties.

Cloud amount feedback (units of $\text{W m}^{-2} \text{K}^{-1}$) can then be finally written as

$$\text{CAF} = \frac{k \Delta c}{\Delta T_s}. \quad (5)$$

The sign convention is that positive values indicate positive cloud amount feedback, which means an amplification

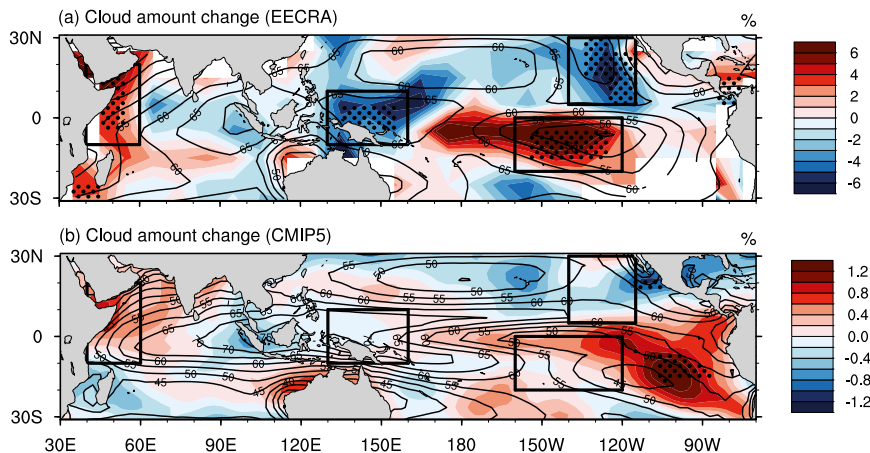


FIG. 1. Total cloud amount change (1954–2005): (a) EECRA and (b) CMIP5 multimodel mean. Contours represent cloud amount climatology (long-term mean), while stippling indicates where the changes are robust. In (a) changes are considered robust if they pass a two tailed Student's t test at the 90% level where the degrees of freedom for the test correspond to the number of observations in each grid box, and are adjusted to take into account autocorrelation at lag1 where the autocorrelation is significant at the 90% level of a Pearson's R test. In (b) stippling indicates where at least 31 models out of 42 (74%) agree on sign. The boxed regions highlight where observed cloud changes are robust.

of climate change, and negative values indicate negative cloud amount feedback, which means a reduction of climate change. We note that since we do not consider vertical changes in cloud cover and cloud properties, our computation of cloud amount feedback is not the same as cloud feedback, which can be written as the sum of cloud amount, cloud altitude, cloud optical feedbacks, and a residual term (Zelinka et al. 2012b).

We estimate cloud amount feedback in models as in observations using Eq. (5). We compute model estimates for the first ensemble member (r1i1p1) of the 42 models considered, and then obtain the multimodel mean by averaging all estimates. Averaging across multiple models ensures better separation of long-term forced climate trends from internal climate variability. Since we subtracted tropical mean cloud amount from cloud fields, both model and observational estimates of cloud amount feedback are relative to the tropical mean. Hence, positive local feedback means more positive than the tropical mean, and negative local feedback more negative than the tropical mean. We note that the tropical multimodel mean cloud change is -0.25% ; therefore, the absolute and relative estimates of local cloud amount feedback in the multimodel mean are not much different from one another and exhibit the same sign. We cannot evaluate the difference between absolute and relative estimates of local cloud amount feedback in observations because of the observational biases discussed above.

4. Results

a. Cloud amount change

Figure 1 shows total cloud amount changes from 1954 to 2005 in (a) observations (EECRA) and (b) the CMIP5 multimodel mean. Contours represent cloud climatology, while stippling indicates where the change is robust. For observations, the change is considered robust where it is significant at the 90% level of a two-tailed Student's t test. The degrees of freedom in each grid box correspond to the number of observations, and are adjusted to take into account autocorrelation at lag 1 where the autocorrelation is significant at the 90% level of a Pearson's R test. For models, stippling indicates where at least 31 out of 42 ($\sim 74\%$) models agree on the sign of cloud change. Figure 1 shows that the tropical pattern of the multimodel mean cloud amount change shares many large-scale features with observations, although changes are smaller (note the different color scales). Observations (Fig. 1a) display robust cloud changes in the four regions contoured by black boxes: cloud cover is found to decrease over the northeast Pacific and equatorial western Pacific, and to increase over the southern central Pacific and western Indian Ocean. Over these regions, the multimodel mean exhibits cloud changes of the same sign as observations but smaller in magnitude (Fig. 1b). In addition, models simulate robust cloud increase over the subtropical southeast Pacific (5° – 20° S, 80° – 120° W), which is the only region where there is good intermodel agreement. While there are not enough observations in EECRA to constrain cloud cover changes

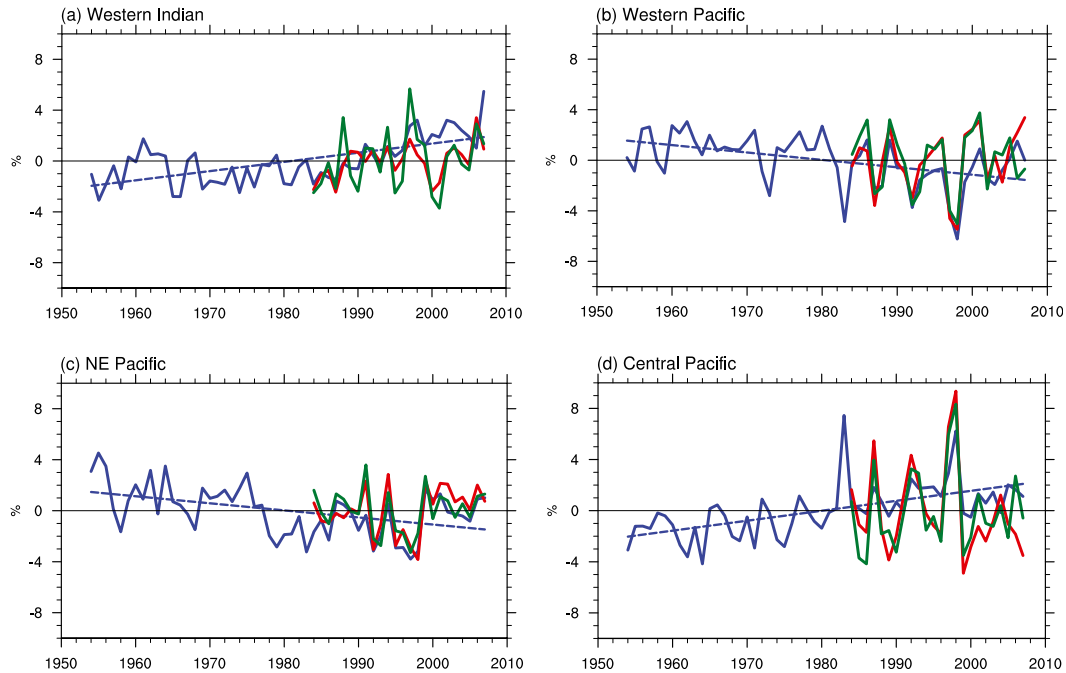


FIG. 2. Regional time series of total cloud amount interannual anomalies in the four boxed regions of Fig. 1. Blue refers to EECRA (1954–2008), red to ISCCP (1984–2007), and green to PATMOS-X (1984–2007). The blue dashed line is the linear trend fitted to EECRA.

over this region, the multimodel mean is consistent with observed positive cloud trends from 1900 to present in the southeast Pacific found in the ICOADS observations by Deser et al. (2010).

To corroborate these long-term cloud changes, we compare cloud anomalies in EECRA with ISCCP and PATMOS-X. Figure 2 shows interannual cloud cover anomalies in the four boxed regions of Fig. 1 where cloud changes in EECRA are statistically significant. EECRA anomalies are plotted in blue, ISCCP in red, and PATMOS-X in green. Dashed blue lines represent the linear trend fit to EECRA anomalies. Cloud anomalies in EECRA show less interannual variance than satellite observations; however, interannual fluctuations and trends are consistent in the three datasets in the overlapping years of coverage (1984–2007). For example, interannual peaks during ENSO events in the western and central Pacific boxes are evident in all three datasets, and decadal fluctuations in cloud cover over the northeast Pacific due to

shifts in the Pacific decadal oscillation (Deser et al. 2004) are also captured by all datasets. In Table 2 we compute correlation coefficients between the time series shown in Fig. 2. All correlations are significant at the 95% level of a two-tailed Pearson’s R test with the exception of the western Indian box where surface observations do not show statically significant correlation with satellites. We note that there is less agreement also between the two satellites in this region.

As discussed above, EECRA observations suffer from global spurious variability, which makes the interpretation of long-term trends problematic. However, consistency with satellite datasets where cloud changes are statistically significant (Fig. 2) gives increased confidence in the credibility of cloud changes in EECRA. The western Indian Ocean is a region where there is less agreement with satellites, and this needs to be taken into account in the interpretation of long-term cloud changes. We note, however, that models simulate consistent sign

TABLE 2. Linear correlation coefficient between the time series shown in Fig. 2. Bolded values indicate where correlations are significant at the 95% level of a Pearson’s R test.

Correlation coefficient	EECRA-ISCCP	EECRA-PATMOSX	ISCCP-PATMOSX
Western Indian	0.24	0.20	0.64
Western Pacific	0.81	0.78	0.79
Northeast Pacific	0.83	0.77	0.82
Central Pacific	0.75	0.78	0.86

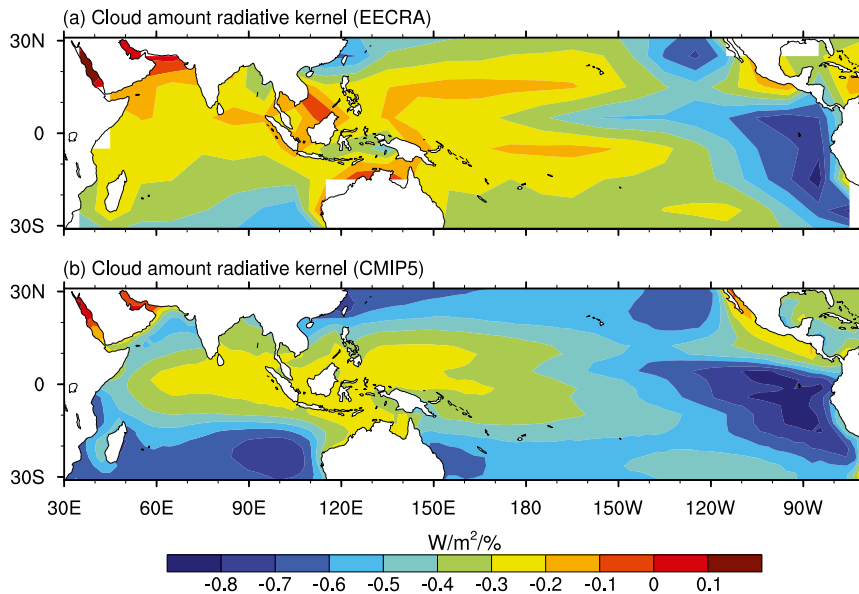


FIG. 3. Cloud amount radiative kernel computed as mean cloud radiative effect (CRE) divided by mean cloud cover. (a) Observational estimate (CRE is from CERES and mean cloud cover is from EECRA) and (b) CMIP5 multimodel mean.

of cloud change with observations over this region and similar large-scale patterns in all the Indo-Pacific Ocean (Fig. 1), which suggests that there could be robust physical mechanisms in models to explain the observed cloud cover changes.

We quantify the radiative impact associated with these long-term cloud trends by computing cloud amount feedback, and then compare observational estimates of cloud amount feedback with those derived in climate models. While satellite products may seem a more reliable dataset to estimate cloud feedbacks, their short-term coverage (less than 30 yr) limits their applicability for climate change studies. In fact, trends in atmospheric variables on time scales of 30 yr or shorter tend to reflect internal climate variability, in particular over regions characterized by high variability on decadal time scales, such as the North Pacific (Deser et al. 2012) and North Atlantic (Ting et al. 2009). For example, cloud signals in the northeast Pacific exhibit significant decadal fluctuations, which are linked to shifts in the Pacific decadal oscillation (PDO) that occurred in the 1976–77 and late 1990s. The time series in Fig. 2c show that all datasets exhibit reduced cloud cover from the mid-1970s to the late 1990s when SST in the eastern Pacific was warmer due to the positive phase of the PDO, and then increased cloud cover from the late 1990s when SST was colder due to the negative phase of the PDO. Therefore, the slightly positive trend in cloud cover from 1984 to 2007 in the northeast Pacific reflects decadal variability and is not representative of the long-term trend in EECRA (blue dashed line in Fig. 2c). This suggests

that satellite cloud products are not suitable for climate change studies in regions where decadal variability is important. For this reason, we choose to estimate long-term cloud amount feedback from ship-based observations, which cover more than five decades and are less sensitive to decadal fluctuations.

b. Cloud amount feedback

To obtain the cloud amount feedback, we multiply cloud amount radiative kernel by cloud cover change and then divide by tropical mean change in SST, as defined in Eq. (5). We first obtain the observational estimate of cloud amount radiative kernel (Fig. 3a), which is computed as the mean cloud radiative effect from CERES divided by the mean cloud cover from EECRA, after regridding CERES to the gridbox size of EECRA. The model estimates of cloud amount radiative kernel are computed as in observations for each of the 42 models. The multimodel mean (Fig. 3b) is then obtained by averaging all model estimates. Figure 3a (observations) and Fig. 3b (models) show good agreement in sign. Negative values indicate where clouds have a net (i.e., shortwave plus longwave) cooling effect, while positive values indicate where clouds have a net warming effect. Cloud amount radiative kernels are negative almost everywhere in both observations and models, which means that clouds have a net cooling effect. Models display even larger values than observations, suggesting that the radiation budget in the models is more sensitive to changes in cloud cover. This is consistent with the fact

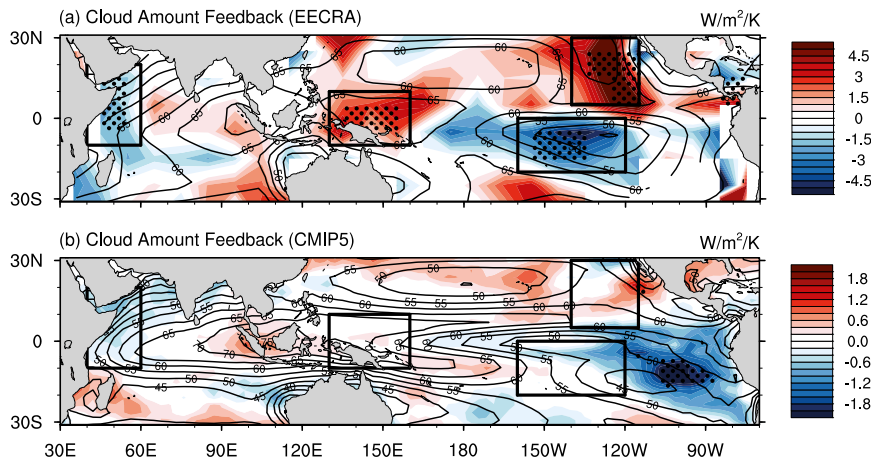


FIG. 4. Cloud amount feedback. (a) Observational estimate computed multiplying cloud amount radiative kernel (Fig. 3a) by EECRA cloud amount changes (Fig. 1a) and then dividing by tropical mean change in SST from HadISST (0.46°C). Contours represent total cloud amount climatology from EECRA. Stippling indicates where cloud amount feedback is robust and is computed as in Fig. 1. (b) CMIP5 multimodel mean. Contours represent the multimodel mean cloud amount climatology. Stippling indicates where at least 31 models out of 42 (~74%) agree on sign. Boxes indicate the regions where cloud changes in Fig. 1a are statistically significant.

that models simulate too few and too bright clouds (Nam et al. 2012), so that the numerator of the cloud amount radiative kernel (i.e., CRE) is too large (negative) while the denominator (i.e., cloud amount) is too small, making the cloud amount radiative kernel larger and more negative in models than in observations. The largest discrepancies between the multimodel mean and observational estimates occur over the central and western tropical Pacific and southern Indian Ocean, where clouds in observations have a smaller cooling effect than in models (Fig. 3).

We note that the observational estimate shown in Fig. 3a is sensitive to cloud climatology. For instance, if we use ISCCP or PATMOS-X instead of EECRA, the cloud amount radiative kernel looks slightly different, although we still get less negative values than the multimodel mean, especially in the western Pacific. These slight differences do not influence our conclusions because we use cloud amount radiative kernel not to evaluate model performance, but rather to weigh the radiative impact of cloud cover changes in relation to the mean cloud cover. For example, if in a particular location of the world cloud cover is larger in ISCCP (e.g., 80%) than in EECRA (e.g., 60%) for the same value of CRE, then a 5% change in cloud cover will have relatively larger impact on cloud amount feedback computed from EECRA than from ISCCP, because the fraction of cloud change to mean cloud cover is larger in EECRA (5%/60%) than ISCCP (5%/80%). The same applies to intermodel differences, although models simulate different cloud climatology due

to different model parameterizations rather than different retrieval methods.

After obtaining the cloud amount radiative kernel, we compute model and observational estimates of cloud amount feedback, which are shown in Fig. 4. Figure 4 is calculated multiplying long-term trends in cloud cover by cloud amount radiative kernel, and then dividing by tropical mean SST change. Model estimates of cloud amount feedback are computed for each model, and then the multimodel mean is obtained by averaging all model estimates. Contours in Fig. 4 represent total cloud cover climatology, while stippling indicates where the changes are statistically significant. Observational cloud amount feedback is statistically significant where cloud trends shown in Fig. 1a are, that is, over the northeast Pacific and western Pacific where cloud amount feedback is positive, and central Pacific and western Indian where cloud amount feedback is negative. Model cloud amount feedback is only significant over the southeast Pacific where there is intermodel agreement in cloud trends. The multimodel mean cloud amount feedback (Fig. 4b) is less than half the observational values (Fig. 4a); nevertheless, the sign of the feedback is consistent with observations over most of the Indian and Pacific Oceans.

Cloud amount feedback [Eq. (5)] can be split into contributions from $1/\Delta T_s$, ΔC , and k . To roughly estimate which of these terms contributes the most to weaker model cloud amount feedback, we compute the fractional change in cloud amount feedback (CAF) in the four boxed regions of Fig. 4. The fractional change

TABLE 3. Observed minus multimodel mean fractional changes of (left) cloud amount radiative kernel k , (middle) cloud cover change ΔC , and (right) tropical mean SST change ΔT_s , in the four boxed regions of Fig. 4. The denominators are mean cloud amount radiative kernel, cloud cover change, and tropical mean SST change from observations. The numbers shown are the absolute values.

Differences between observations and the multimodel mean	$\delta k/k$	$\delta \Delta C/\Delta C$	$\delta \Delta T_s/\Delta T_s$
Western Indian	0.70	0.89	0.24
Western Pacific	0.41	1.00	"
Northeast Pacific	0.16	0.96	"
Central Pacific	0.72	0.91	"

in CAF can be written as $\delta \text{CAF}/\text{CAF} = (\delta k/k) + (\delta \Delta C/\Delta C) - (\delta \Delta T_s/\Delta T_s)$, where δ represents the differences between observed and multimodel mean values. We do not expect the LHS of this equation to be equal to the difference between the computed multimodel mean and observations because this equation is a valid approximation only for small perturbations. Nonetheless, this approximation indicates which terms contribute the most to the differences between models and observations. The fractional changes of the RHS terms of the equation are reported in Table 3, which shows that the largest contribution to weaker model cloud amount feedback comes from smaller model-simulated cloud cover changes than observed.

Figures 5 and 6 show the estimates of cloud amount feedback in the four boxed regions of Fig. 4 in each model (numbered bars), multimodel mean (denoted M), and observations (OBS). Numbered bars correspond to individual model estimates according to the legend in Table 4. Figure 5 shows the estimates in the (a) western Indian and (b) western Pacific, while Fig. 6 shows the (a) northeast Pacific and (b) central Pacific. Also plotted in Figs. 5 and 6 are estimates of observational errors (horizontal lines), which represent the error on the estimates of cloud trends (see the caption of Fig. 5). While

generally the multimodel mean is significantly smaller than observations, models individually can simulate cloud amount feedback of the same strength if not larger than observations. In the western Indian (Fig. 5a), 30 models out of 42 (~71%) agree in sign with observations. Of these, 10 fall within the error range of observations, and 2 exceed the upper extent of the error range. In the western Pacific (Fig. 5b), 24 models (~57%) agree in sign with observations, 8 fall within the error range, and 1 exceeds the upper extent of the error range. In the northeast Pacific (Fig. 6a), 21 models (50%) agree in sign with observations, and only 1 falls within the error range. In the central Pacific (Fig. 6b), 25 models (~59%) agree with observations, 3 fall within the error range, and 1 exceeds the upper extent of the error range. The region of largest uncertainty is therefore the northeast Pacific, which is a region predominantly covered by low-level marine stratocumulus clouds. It is also noteworthy that the observational estimate in the northeast Pacific is larger than that simulated by any models, whereas this is not the case for the other regions, where some of the model estimates can exceed the observed changes.

We computed similar bar charts for changes in cloud cover in these four regions. No model simulated cloud cover changes larger than the observed in any of the regions (not shown). Therefore, some models are able to simulate similar magnitude cloud amount feedback as observations (Fig. 5 and 6), not because they reproduce the same cloud amount changes but because they overestimate the radiative effect of clouds (Fig. 3). We do not find any particular model that performs better than the others in the simulation of cloud cover changes or cloud amount feedback in all four regions.

We mentioned that total cloud fraction computed in the models is not the same as observed total cloud fraction, which introduces uncertainty in the estimates of cloud amount feedback. However, the uncertainty in the estimation of cloud amount feedback due to the different

TABLE 4. Legend of model numbers for Figs. 5 and 6.

1. ACCESS1-0	15. GFDL-CM3	29. MIROC-ESM-CHEM
2. ACCESS1-3	16. GFDL-ESM2G	30. MIROC-ESM
3. BNU-ESM	17. GFDL-ESM2M	31. MIROC4h
4. CCSM4	18. GISS-E2-H-CC	32. MIROC5
5. CESM1-BGC	19. GISS-E2-H	33. MPI-ESM-LR
6. CESM1-CAM5	20. GISS-E2-R-CC	34. MPI-ESM-MR
7. CESM1-FASTCHEM	21. GISS-E2-R	35. MPI-ESM-P
8. CESM1-WACCM	22. HadCM3	36. MRI-CGCM3
9. CNRM-CM5-2	23. HadGEM2-AO	37. MRI-ESM1
10. CNRM-CM5	24. HadGEM2-CC	38. NorESM1-ME
11. CSIRO-Mk3-6-0	25. HadGEM2-ES	39. NorESM1-M
12. CanESM2	26. IPSL-CM5A-LR	40. BCC-CSM1-1-M
13. FGOALS-g2	27. IPSL-CM5A-MR	41. BCC-CSM1-1
14. FIO-ESM	28. IPSL-CM5B-LR	42. INM-CM4

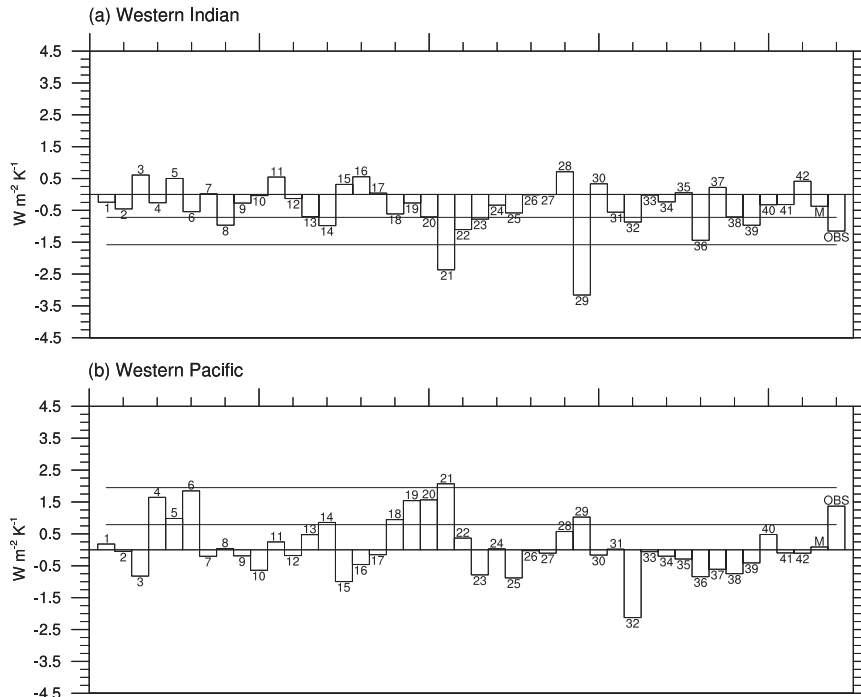


FIG. 5. Cloud amount feedback averaged over the first two boxed regions of Fig. 4: (a) western Indian and (b) western Pacific. The numbers indicate the model name (see legend in Table 4). Horizontal lines represent the estimated range of observational errors, which are computed using the propagation of uncertainty formula assuming that the error in the estimate of cloud amount change is much larger than the errors in the estimates of tropical mean SST change and cloud amount radiative kernel. The observational error on cloud amount feedback (CAF) can therefore be written as $\sigma_{CAF}/CAF = \sigma_{\Delta c}/\Delta C$. From Eq. (4), $CAF = k\Delta c/\Delta T_s$; therefore, $\sigma_{CAF} = \sigma_{\Delta c}(k/\Delta T_s)$, where k is averaged over the boxed region and ΔT_s is the tropical mean SST change ($0.46^{\circ}C$); also, $\sigma_{\Delta c}$ represents the 90% confidence range and is computed as the standard error on the estimate of the cloud amount trend multiplied by the t value at the 90% probability level of a two-tailed Student's t test with degrees of freedom equal to the number of observations adjusted to account for the autocorrelation at lag 1.

definitions of total cloud fraction in models and observations (Marchand et al. 2010) seems to be much smaller than the uncertainty that arises from the large intermodel spread in the simulation of cloud cover changes and cloud amount feedback (Figs. 5 and 6).

5. Discussion

The pattern of observed cloud cover changes over the tropical Pacific Ocean (Fig. 1) for the years 1954–2005 is similar to century time scale cloud cover changes (1900 to the present) computed from ICOADS (Deser et al. 2010). Those authors argued that the pattern in Fig. 1a is reminiscent of El Niño because there is decrease in cloud cover over the western Pacific and increase over the central Pacific. They found that this El Niño-like cloud change pattern in the western Pacific was consistent with an observed eastward shift in precipitation in the tropical Pacific and weakening of the Walker circulation over the

last century (Vecchi et al. 2006). Furthermore, Tokinaga et al. (2012) ran AGCM experiments with prescribed SST patterns from observations and showed that the models were able to reproduce cloud cover changes consistent with Fig. 1a, along with an eastward shift in convection and weakening of the Walker circulation. Thus, the east-west dipole pattern of cloud change and feedback in the central and western Pacific may be explained by El Niño-like mechanisms occurring on long time scales.

On the other hand, cloud increase in the southeast Pacific subtropical stratocumulus and trade-cumulus regions shown by both Fig. 1b of this study and Deser et al. (2010) does not resemble cloud changes during El Niño events, because during El Niño events cloud cover decreases over both the southeast and northeast Pacific stratocumulus regions (Deser et al. 2004). This suggests that, in contrast to the western and central Pacific, mechanisms of climate change in the eastern Pacific might not be explained by El Niño-like mechanisms (cf. DiNezio et al. 2009).

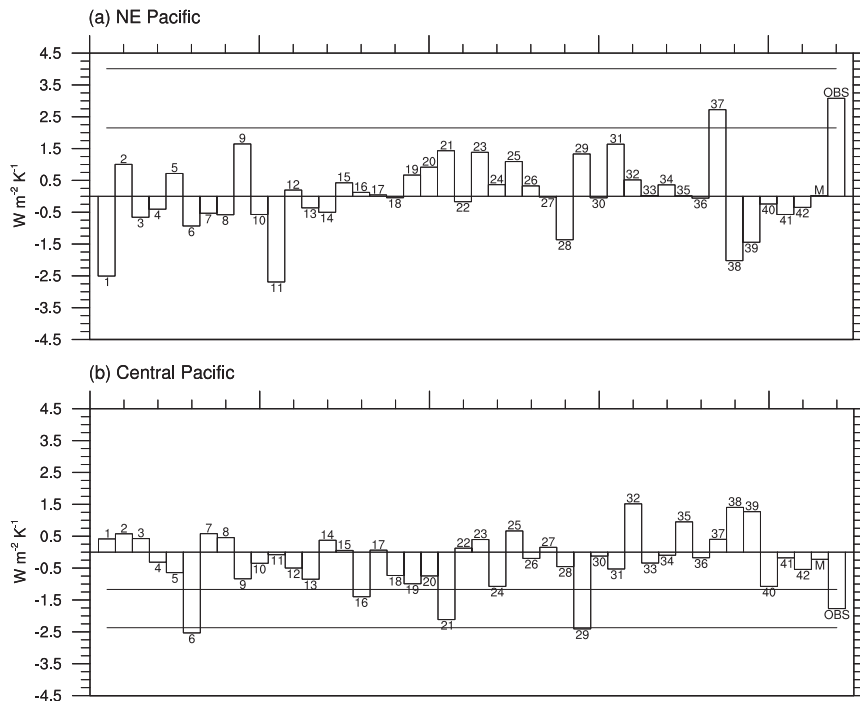


FIG. 6. As in Fig. 5, but for cloud amount feedback averaged over the other two boxes regions of Fig. 4: (a) northeast Pacific and (b) central Pacific.

The decrease in cloud amount and the resulting positive cloud amount feedback over the northeast Pacific stratocumulus region is instead consistent with a stratocumulus-to-cumulus (Sc-to-Cu) transition hypothesis (Bretherton and Wyant 1997). Eastman et al. (2011) used the same dataset (EECRA) as in the present study to look at changes in low-level cloud types over the years 1954–2008. They found an increase in the frequency of occurrence in cumulus and a decrease in stratocumulus in the northeast Pacific and other subtropical stratocumulus regions, which suggests a long-term Sc-to-Cu transition. Cumulus cloud cover is more scattered than stratocumulus, so therefore cloud fraction decreases during the transition resulting in positive cloud amount feedback.

The only region where there is intermodel agreement in cloud amount changes is the southeast Pacific, where cloud amount increases in the historical simulations. The subtropical southeast Pacific is a region where models robustly simulate a minimum in SST warming in response to climate change (Xie et al. 2010; DiNezio et al. 2011). This minimum warming has usually been explained as arising from a strengthening of the trade winds (Falvey and Garreaud 2009). Our results suggest that negative cloud amount feedback in the southeast Pacific could contribute as well to enhance this minimum warming.

The observed and simulated changes in cloud amount feedback are consistent with some of the mechanisms

explaining climate change cloud feedbacks in doubled- CO_2 (Zelinka et al. 2012b) and abrupt CO_2 quadrupling GCM experiments (Zelinka et al. 2013). Zelinka et al. (2012b) split cloud feedback into contributions from cloud amount, cloud altitude, and cloud optical depth feedbacks. As in our study, they found a negative cloud amount feedback over the central Pacific due to an increase in cloud amount. This negative cloud amount feedback, however, was largely compensated by a positive cloud altitude feedback, resulting in net positive cloud feedback over the central Pacific. Their results were consistent with the hypothesis of fixed-anvil-temperature of Hartmann and Larson (2002), according to which high-level clouds in the tropics tend to rise as the climate warms to conserve their cloud-top temperature. Our findings support the cloud amount feedback part of this mechanism. Over the northeast Pacific, Zelinka et al. (2012b) found positive cloud amount feedback as in our study. They also found positive cloud altitude feedback, which along with positive cloud amount feedback is consistent with the Sc-to-Cu transition hypothesis and deepening of the marine boundary layer in response to warmer SST.

The complexity of the mechanisms involved in cloud changes, which is reflected by the observed north–south and east–west asymmetries, suggests that regional differences in mechanisms of cloud change need to be

taken into account. Since observed cloud–environment relationships are similar in all subtropical stratocumulus regions on interannual time scales (e.g., Klein and Hartmann 1993), some studies have suggested using composites of cloud cover changes to explore mechanisms of cloud change in regions characterized by the same large-scale subsidence rates such as the northeast and southeast subtropical stratocumulus regions (Bony et al. 2004). While this technique has improved our understanding of the relative roles of the thermodynamic and dynamic components of cloud changes under idealized climate change scenarios (e.g., Bony et al. 2004; Briant and Bony 2013), our results suggest that mechanisms of cloud changes need to be studied regionally. In fact, environmental conditions (e.g., SST, SLP, large-scale subsidence, precipitation) can respond differently to climate change in regions characterized by the same large-scale subsidence regime (e.g., Vecchi and Soden 2007a). Regional differences can be therefore very large, even within the same dynamic regime.

Soden and Vecchi (2011) showed that the subtropical stratocumulus regions are among the regions of largest intermodel disagreement in cloud feedback. Three of the subtropical stratocumulus regions identified by Klein and Hartmann (1993) are located in the Indo-Pacific Ocean (northeast and southeast Pacific, and southeast Indian). In this study we provide observational support for positive cloud amount feedback relative to the tropical mean over the northeast Pacific from the second half of the twentieth century. We find positive but not statistically significant cloud amount feedback over the southeast Indian Ocean. Over the southeast Pacific, instead, cloud cover is found to increase in both observations (Deser et al. 2010) and climate models (Fig. 1b), suggesting negative cloud amount feedback, but there are not sufficient data in EECRA to estimate cloud amount feedback in this region.

We finally note that cloud feedback has been historically defined as the cloud-induced change in TOA radiation per unit change in SST, all else being equal. To diagnose cloud feedback, idealized model experiments in which the only variable that is changing is SST (e.g., perturbed SST experiments) or the CO₂ concentration (e.g., abrupt 4×CO₂ experiments) are commonly used. In our study, however, we examine historical simulations and observations. In these experiments and in the real world cloud cover is also responding to changing in other variables in addition to planetary warming—for example, changes in anthropogenic aerosols, which have direct and indirect effects on clouds (cf. Booth et al. 2012; Allen et al. 2012), and the ozone hole (Grise et al. 2013), which along with changes in aerosols has affected the large-scale atmospheric circulation and therefore

cloud patterns in ways that differ from the response to an increase in SST alone. Moreover, trends may be influenced by the timing of ENSO or other sources of internal climate variability, thereby giving a single estimate of cloud feedback that is valid, but possibly biased on one direction or another relative to the “true” value.

We are unable to separate the temperature-mediated cloud changes (those that feed back on the warming) from those cloud changes that arise due to other forcing agents included in the historical runs and observations. Nevertheless, some large-scale features such as an east–west asymmetry in the western Pacific, positive cloud amount feedback in the northeast Pacific, and the robust negative cloud amount feedback in the southeast Pacific, are also simulated by idealized climate change experiments (Zelinka et al. 2012b; Soden and Vecchi 2011), which suggests that some of the mechanisms explaining cloud changes in idealized increasing CO₂ experiments may be already evident in the available observations.

6. Conclusions

In this study we have examined the problem of constraining cloud feedback in climate models by taking a long-term perspective from cloud observations. Synoptic reports of cloud cover from ships contained in the EECRA dataset are the longest record of cloud information over the ocean, and could potentially be used to constrain cloud feedback in climate models. To remove spurious variability in this dataset, we subtracted the annual tropical mean from each grid box. Then, we compared the corrected interannual cloud cover anomalies with two satellite products (ISCCP and PATMOS-X), from which the tropical mean was also removed. During the overlapping years of coverage, EECRA and the two satellites showed good degree of agreement over most part of the Indian and Pacific Oceans, although a reduced degree of agreement was found in the western Indian Ocean among all datasets.

We showed that long-term cloud changes relative to the tropical mean in EECRA were similar to the multimodel mean of 42 CMIP5 historical simulations over the years 1954–2005 but smaller in magnitude. Models and observations displayed a north–south asymmetry in cloud change in the eastern Pacific, with decreases in cloud cover over the northeast Pacific and increases over the central and southeast Pacific, and an east–west dipole, with decreases in cloud cover over the equatorial western Pacific, and increases over the central Pacific. The east–west dipole in the western Pacific is reminiscent of cloud cover changes during El Niño events, and consistent with eastward shift in precipitation and

reduced strength of the Walker circulation observed over the last century.

We estimated cloud amount feedback relative to the tropical mean associated with these cloud changes. Observational estimates showed statistically significant cloud amount feedback over four regions: cloud amount feedback was found to be positive over the northeast Pacific subtropical stratocumulus region and equatorial western Pacific, and negative over the southern central Pacific and western Indian. Compared to observations, the multimodel mean displayed consistent but weaker cloud amount feedback over these regions and similar large-scale features. Although the multimodel mean was found to be significantly smaller than in observations, some models simulated cloud amount feedback of the same strength if not stronger than in observations.

We proposed a method to estimate cloud amount feedback that can be easily used to compare models with observations. As more years of data from satellite-based cloud observations become available, this method can be used to corroborate the observational estimates of cloud amount feedback provided here. Finally, since climate models and observations showed similar large-scale patterns of cloud changes, we suggest that mechanisms responsible for cloud changes in models could help explain the observed changes.

Acknowledgments. We thank Mark Zelinka and an anonymous reviewer for their insightful revisions. We acknowledge the World Climate Research Programme's Working Group on Coupled Modeling, which is responsible for CMIP5, and we thank the climate modeling groups (listed in Table 1 of this paper) for producing and making available their model output. The free software NCAR Command Language (version 6.0.0) was used to create the plots and analyze data. We are also grateful to Paquita Zuidema, Rob Burgman, and Ben Kirtman for their insights. This work is supported by the Office of Science, U.S. DOE (Grant DESC0004897), the NSF Climate and Large-scale Dynamics Program (Grant AGS0946225), and the NOAA Climate Program Office (Grant NA10OAR4310204).

REFERENCES

- Albrecht, B. A., C. S. Bretherton, D. Johnson, W. H. Schubert, and A. S. Frisch, 1995: The Atlantic Stratocumulus Transition Experiment—ASTEX. *Bull. Amer. Meteor. Soc.*, **76**, 889–904.
- Allen, R. J., S. C. Sherwood, J. R. Norris, and C. S. Zender, 2012: Recent Northern Hemisphere tropical expansion primarily driven by black carbon and tropospheric ozone. *Nature*, **485**, 350–354, doi:10.1038/nature11097.
- Bony, S., and J.-L. Dufresne, 2005: Marine boundary layer clouds at the heart of tropical cloud feedback uncertainties in climate models. *Geophys. Res. Lett.*, **32**, L20806, doi:10.1029/2005GL023851.
- , —, H. LeTreut, J.-J. Morcrette, and C. Senior, 2004: On dynamic and thermodynamic components of cloud changes. *Climate Dyn.*, **22**, 71–86.
- , and Coauthors, 2006: How well do we understand and evaluate climate change feedback processes? *J. Climate*, **19**, 3445–3482.
- Booth, B. B. B., N. J. Dunstone, P. R. Halloran, T. Andrews, and N. Bellouin, 2012: Aerosols implicated as a prime driver of twentieth-century North Atlantic climate variability. *Nature*, **484**, 228–232.
- Bretherton, C. S., and M. C. Wyant, 1997: Moisture transport, lower-tropospheric stability, and decoupling of cloud-topped boundary layers. *J. Atmos. Sci.*, **54**, 148–167.
- Brient, F., and S. Bony, 2013: Interpretation of the positive low-cloud feedback predicted by a climate model under global warming. *Climate Dyn.*, **40**, 2415–2431, doi:10.1007/s00382-011-1279-7.
- Clement, A. C., R. Burgman, and J. R. Norris, 2009: Observational and model evidence for positive low-level cloud feedback. *Science*, **325**, 460–464.
- Deser, C., A. S. Phillips, and J. W. Hurrell, 2004: Pacific interdecadal climate variability: Linkages between the tropics and the North Pacific during boreal winter since 1900. *J. Climate*, **17**, 3109–3124.
- , —, and M. A. Alexander, 2010: Twentieth century tropical sea surface temperature trends revisited. *Geophys. Res. Lett.*, **37**, L10701, doi:10.1029/2010GL043321.
- , A. Phillips, V. Bourdette, and H. Teng, 2012: Uncertainty in climate change projections: The role of internal variability. *Climate Dyn.*, **38**, 527–546.
- DiNezio, P., A. Clement, G. A. Vecchi, B. Soden, B. Kirtman, and S.-K. Lee, 2009: Climate response of the equatorial Pacific to global warming. *J. Climate*, **22**, 4873–4892.
- , —, —, —, A. J. Broccoli, B. L. Otto-Bliessner, and P. Braconnot, 2011: The response of the Walker circulation to Last Glacial Maximum forcing: Implications for detection in proxies. *Paleoceanography*, **26**, PA3217, doi:10.1029/2010PA002083.
- Dufresne, J.-L., and S. Bony, 2008: An assessment of the primary sources of spread of global warming estimates from coupled atmosphere–ocean models. *J. Climate*, **21**, 5135–5144.
- Eastman, R., S. G. Warren, and C. J. Hahn, 2011: Variations in cloud cover and cloud types over the Ocean from surface observations, 1954–2008. *J. Climate*, **24**, 5914–5934.
- Evan, A. T., A. K. Heidinger, and D. J. Vimont, 2007: Arguments against a physical long-term trend in global ISCCP cloud amounts. *Geophys. Res. Lett.*, **34**, L04701, doi:10.1029/2006GL028083.
- , R. J. Allen, R. Bennartz, and D. J. Vimont, 2013: The modification of sea surface temperature anomaly linear damping time scales by stratocumulus clouds. *J. Climate*, **26**, 3619–3630.
- Falvey, M., and R. D. Garreaud, 2009: Regional cooling in a warming world: Recent temperature trends in the southeast Pacific and along the west coast of subtropical South America (1979–2006). *J. Geophys. Res.*, **114**, D04102, doi:10.1029/2008JD010519.
- Grise, K. M., L. M. Polvani, G. Tselioudis, Y. Wu, and M. D. Zelinka, 2013: The ozone hole indirect effect: Cloud-radiative anomalies accompanying the poleward shift of the eddy-driven jet in the Southern Hemisphere. *Geophys. Res. Lett.*, **40**, 3688–3692, doi:10.1002/grl.50675.

- Hahn, C. J. and S. G. Warren, 1999: Extended edited synoptic cloud reports from ships and land stations over the globe, 1952–1996. Carbon Dioxide Information Analysis Center Rep. CDIA/NDP-026C, doi:10.3334/CDIAC/cli.ndp026c.
- , and —, 2009: Extended edited synoptic cloud reports from ships and land stations over the globe, 1952–1996 (2009 update). Carbon Dioxide Information Analysis Center Numerical Data Package NDP-026C, 79 pp, doi:10.3334/CDIAC/cli.ndp026c.
- Hartmann, D. L., and K. Larson, 2002: An important constraint on tropical cloud–climate feedback. *Geophys. Res. Lett.*, **29**, 1951, doi:10.1029/2002GL015835.
- Jacobowitz, H., L. L. Stowe, G. Ohring, A. Heidinger, K. Knapp, and N. R. Nalli, 2003: The Advanced Very High Resolution Radiometer Pathfinder Atmosphere (PATMOS) climate dataset: A resource for climate research. *Bull. Amer. Meteor. Soc.*, **84**, 785–793.
- Klein, S. A., and D. L. Hartmann, 1993: The seasonal cycle of low stratiform clouds. *J. Climate*, **6**, 1587–1606.
- , —, and J. R. Norris, 1995: On the relationships among low-cloud structure, sea surface temperature, and atmospheric circulation in the summertime northeast Pacific. *J. Climate*, **8**, 1140–1155.
- , Y. Zhang, M. D. Zelinka, R. Pincus, J. Boyle, and P. J. Gleckler, 2013: Are climate model simulations of clouds improving? An evaluation using the ISCCP simulator. *J. Geophys. Res.*, **118**, 1329–1342, doi:10.1002/jgrd.50141.
- Loeb, N. G., B. A. Wielicki, D. R. Doelling, G. L. Smith, D. F. Keyes, S. Kato, N. Manalo-Smith, and T. Wong, 2009: Toward optimal closure of the Earth's top-of-atmosphere radiation budget. *J. Climate*, **22**, 748–766.
- Marchand, R., T. Ackerman, M. Smyth, and W. B. Rossow, 2010: A review of cloud top height and optical depth histograms from MISR, ISCCP, and MODIS. *J. Geophys. Res.*, **115**, D16206, doi:10.1029/2009JD013422.
- Mauger, G., and J. R. Norris, 2010: Assessing the impact of meteorological history on subtropical cloud fraction. *J. Climate*, **23**, 2926–2940.
- Medeiros, B., B. Stevens, I. M. Held, M. Zhao, D. L. Williamson, J. G. Olson, and C. S. Bretherton, 2008: Aquaplanets, climate sensitivity, and low clouds. *J. Climate*, **21**, 4974–4991.
- Miller, R. L., 1997: Tropical thermostats and low cloud cover. *J. Climate*, **10**, 409–440.
- Muñoz, R., R. Zamora, and J. Rutllant, 2011: The coastal boundary layer at the eastern margin of the southeast Pacific (23.4°S, 70.4°W): Cloudiness-conditioned climatology. *J. Climate*, **24**, 1013–1033.
- Myers, T., and J. Norris, 2013: Observational evidence that enhanced subsidence reduces subtropical marine boundary layer cloudiness. *J. Climate*, **26**, 7507–7524.
- Nam, C., S. Bony, J. L. Dufresne, and H. Chepfer, 2012: The “too few, too bright” tropical low-cloud problem in CMIP5 models. *Geophys. Res. Lett.*, **39**, L21801, doi:10.1029/2012GL053421.
- Norris, J. R., 1998: Low cloud type over the ocean from surface observations. Part II: Geographical and seasonal variations. *J. Climate*, **11**, 383–403.
- , 1999: On trends and possible artifacts in global ocean cloud cover between 1952 and 1995. *J. Climate*, **12**, 1864–1870.
- , 2005: Multidecadal changes in near-global cloud cover and estimated cloud cover radiative forcing. *J. Geophys. Res.*, **110**, D08206, doi:10.1029/2004JD005600.
- Pavolonis, M. J., A. K. Heidinger, and T. Uttal, 2005: Daytime global cloud typing from AVHRR and VIIRS: Algorithm description, validation, and comparisons. *J. Appl. Meteor.*, **44**, 804–826.
- Pincus, R., S. Platnick, S. A. Ackerman, R. S. Hemler, and R. J. P. Hofmann, 2012: Reconciling simulated and observed views of clouds: MODIS, ISCCP, and the limits of instrument simulators. *J. Climate*, **25**, 4699–4720.
- Rayner, N. A., and Coauthors, 2003: Global analyses of sea surface temperature, sea ice, and night marine air temperature since the late nineteenth century. *J. Geophys. Res.*, **108**, 4407, doi:10.1029/2002JD002670.
- Ringer, M. A., and Coauthors, 2006: Global mean cloud feedbacks in idealized climate change experiments. *Geophys. Res. Lett.*, **33**, L07718, doi:10.1029/2005GL025370.
- Rossow, W. B., and R. A. Schiffer, 1999: Advances in understanding clouds from ISCCP. *Bull. Amer. Meteor. Soc.*, **80**, 2261–2287.
- Sandu, I., and B. Stevens, 2011: On the factors modulating the stratocumulus to cumulus transitions. *J. Atmos. Sci.*, **68**, 1865–1881.
- Soden, B. J., and I. M. Held, 2006: An assessment of climate feedbacks in coupled ocean–atmosphere models. *J. Climate*, **19**, 3354–3360.
- , and G. A. Vecchi, 2011: The vertical distribution of cloud feedback in coupled ocean–atmosphere models. *Geophys. Res. Lett.*, **38**, L12704, doi:10.1029/2011GL047632.
- , I. M. Held, R. C. Colman, K. M. Shell, J. T. Kiehl, and C. A. Shields, 2008: Quantifying climate feedbacks using radiative kernels. *J. Climate*, **21**, 3504–3520.
- Solomon, S., D. Qin, M. Manning, Z. Chen, M. Marquis, K. Averyt, M. M. B. Tignor, and H. L. Miller Jr., 2007: *Climate Change 2007: The Physical Science Basis*. Cambridge University Press, 996 pp.
- Stephens, G. L., 2005: Cloud feedbacks in the climate system: A critical review. *J. Climate*, **18**, 237–273.
- Stevens, B., A. Beljaars, S. Bordoni, C. Holloway, M. Köhler, S. Krueger, V. Savijovcic, and Y. Zhang, 2007: On the structure of the lower troposphere in the summertime stratocumulus regime of the northeast Pacific. *Mon. Wea. Rev.*, **135**, 985–1005.
- Taylor, K. E., M. Crucifix, P. Braconnot, C. D. Hewitt, C. Doutriaux, A. J. Broccoli, J. F. B. Mitchell, and M. J. Webb, 2007: Estimating shortwave radiative forcing and response in climate models. *J. Climate*, **20**, 2530–2543.
- , R. J. Stouffer, and G. A. Meehl, 2012: An overview of CMIP5 and the experiment design. *Bull. Amer. Meteor. Soc.*, **93**, 485–498.
- Ting, M. F., Y. Kushnir, R. Seager, and C. H. Li, 2009: Forced and internal twentieth-century SST trends in the North Atlantic. *J. Climate*, **22**, 1469–1481.
- Tokinaga, H., S.-P. Xie, C. Deser, Y. Kosaka, and Y. M. Okumura, 2012: Slowdown of the Walker circulation driven by tropical Indo-Pacific warming. *Nature*, **491**, 439–443, doi:10.1038/nature11576.
- Trenberth, K. E., and J. T. Fasullo, 2009: Global warming due to increasing absorbed solar radiation. *Geophys. Res. Lett.*, **36**, L07706, doi:10.1029/2009GL037527.
- Vecchi, G. A., and B. J. Soden, 2007a: Global warming and the weakening of the tropical circulation. *J. Climate*, **20**, 4316–4340.
- , and —, 2007b: Increased tropical Atlantic wind shear in model projections of global warming. *Geophys. Res. Lett.*, **34**, L08702, doi:10.1029/2006GL028905.
- , —, A. T. Wittenberg, I. M. Held, A. Leetmaa, and M. J. Harrison, 2006: Weakening of tropical Pacific atmospheric

- circulation due to anthropogenic forcing. *Nature*, **441**, 73–76, doi:10.1038/nature04744.
- Webb, M. J., and Coauthors, 2006: On the contribution of local feedback mechanisms to the range of climate sensitivity in two GCM ensembles. *Climate Dyn.*, **27**, 17–38.
- Wood, R., and C. S. Bretherton, 2004: Boundary layer depth, entrainment, and decoupling in the cloud-capped subtropical and tropical marine boundary layer. *J. Climate*, **17**, 3576–3588.
- , and —, 2006: On the relationship between stratiform low cloud cover and lower-tropospheric stability. *J. Climate*, **19**, 6425–6432.
- Woodruff, S. D., H. F. Diaz, S. J. Worley, R. W. Reynolds, and S. J. Lubker, 2005: Early ship observational data and ICOADS. *Climatic Change*, **73**, 169–194.
- , and Coauthors, 2011: ICOADS release 2.5: Extensions and enhancements to the surface marine meteorological archive. *Int. J. Climatol.*, **31**, 951–967.
- Xie, S. P., C. Deser, G. A. Vecchi, J. Ma, H. Teng, and A. T. Wittenberg, 2010: Global warming pattern formation: Sea surface temperature and rainfall. *J. Climate*, **23**, 966–986.
- Zelinka, M. D., and D. L. Hartmann, 2010: Why is longwave cloud feedback positive? *J. Geophys. Res.*, **115**, D16117, doi:10.1029/2010JD013817.
- , and —, 2011: The observed sensitivity of high clouds to mean surface temperature anomalies in the tropics. *J. Geophys. Res.*, **116**, D23103, doi:10.1029/2011JD016459.
- , S. A. Klein, and D. L. Hartmann, 2012a: Computing and partitioning cloud feedbacks using cloud property histograms. Part I: Cloud radiative kernels. *J. Climate*, **25**, 3715–3735.
- , —, and —, 2012b: Computing and partitioning cloud feedbacks using cloud property histograms. Part II: Attribution to changes in cloud amount, altitude, and optical depth. *J. Climate*, **25**, 3736–3754.
- , —, K. E. Taylor, T. Andrews, M. J. Webb, J. M. Gregory, and P. M. Forster, 2013: Contributions of different cloud types to feedbacks and rapid adjustments in CMIP5. *J. Climate*, **26**, 5007–5027.
- Zhou, C., M. D. Zelinka, A. E. Dessler, and P. Yang, 2013: An analysis of the short-term cloud feedback using MODIS data. *J. Climate*, **26**, 4803–4815.